Journal of Solid Mechanics and Materials Engineering

Vol. 2, No. 11, 2008

Maximum Stress for Shrink Fitting System Used for Ceramics Conveying Rollers*

Nao-Aki NODA **, Hendra **, Yasushi TAKASE **
and Masakazu TSUYUNARU **
** Department of Mechanical and Control Engineering, Kyushu Institute of Technology
Sensui-Cho 1-1 Tobata-Ku, Kitakyushu-Shi, Fukuoka, Japan
E-mail: noda@mech.kyutech.ac.jp

Abstract

Steel conveying rollers used in hot rolling mills must be changed very frequently at great cost because hot conveyed strips induce wear on the roller surface in short periods. In this study new roller is considered where a ceramics sleeve is connected with two short shafts at both ends by shrink fitting. Here, the ceramics sleeve may provide longer life and reduces the cost for the maintenance. However, care should be taken for maximum tensile stress appearing between the sleeve and shaft because the fracture toughness of ceramics is extremely lower than the values of steel. In this study FEM analysis is applied to the new structure, and the maximum tensile stress has been investigated with varying the dimensions of the structure. It is found that the maximum tensile stress appearing at the end of sleeves takes a minimum value at a certain amount of shrink fitting ratio.

Key words: Contact Problem, Ceramics, Elasticity, Bending, Finite Element Method

1. Introduction

Cast iron and steel conveying rollers used in hot rolling mills (see Fig.1) must be changed very frequently because hot conveyed strips induce wear on the roller surface in short period. The damage portions are usually repaired using the flame spray coating [1]. Use of ceramics and cemented carbide has been also promoted [2] because they have high temperature resistance and high abrasion resistance.

Figure 2(a) shows the structure of the conventional rollers. For conventional rollers, material consumptions are large and the exchange cost is high because we have to change whole roller. In this study, we will focus on the roller structure where a sleeve and two short shafts are connected by shrink fitting at both ends as shown in Fig.2 (b).

*Received 12 Aug., 2008 (No. T2-08-7001)
Japanese Original : Trans. Jpn. Soc. Mech. Eng., Vol. 74, No. 743, A (2008), pp.919-925 (Received 17 Jan., 2008)
[DOI: 10.1299/jmmp.2.1410]

The new roller is suitable for maintenance and reducing the cost because we can exchange the sleeve only. In addition, the running speed of the steel strip can be changed smoothly due to the light weight. Moreover, further cost reduction can be realized if ceramics are used as the sleeve because they offer high temperature resistance and high abrasion resistance. However, for the hollow rollers, care should be taken for maximum tensile stresses appearing at the edge of the sleeve. In particular, because fracture toughness of ceramics is extremely smaller compared with the values of steel, stress analysis for the roller becomes more and more important. Therefore, in this study FEM analysis will be applied to the structure as shown in Fig.2 (b), and suitable dimensions will be considered.

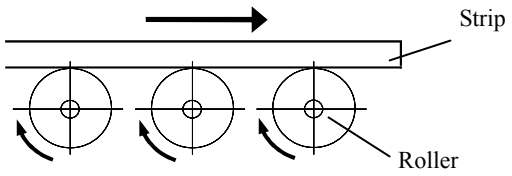

Fig.1 Layout of Conveying Rollers

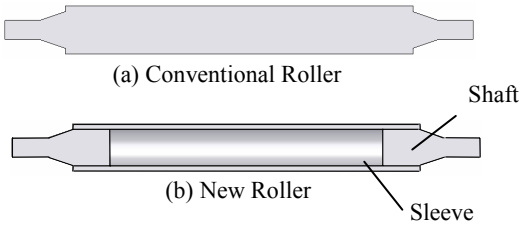

Fig.2 Roller Structure

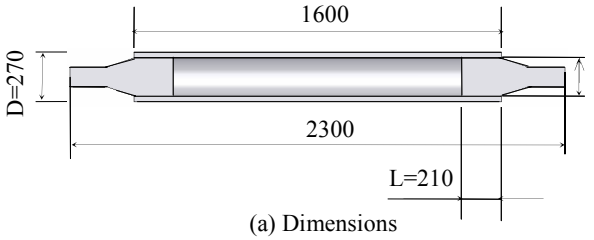

(a) Dimensions

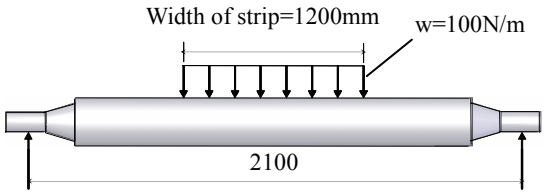

(b) Distributed load

Fig.3 Models considered (mm)

2. Analytical Conditions

Define the shrink fitting ratio as δ/d, where δ is the diameter difference with the diameter $d = 210mm$. Assume that the roller is subjected to distributed load $w = 100N/mm$ and simply supported at both ends (see Fig.3). The friction coefficient between sleeve and shafts is assumed as 0.3.

Table 1 shows the material properties of steel, ceramics and cemented carbide. Stainless steel is usually used for conventional rollers but ceramics and cemented carbide rollers may

provide a longer maintenance span due to their high temperature resistance and high abrasion resistance.

Figure 4 shows the finite element mesh model of the conveying rollers. The total number of elements is 22,340 and the total number of nodes is 26,751. The model of 1/4 of the roller is considered due to symmetry.

3. Results and Discussion

3.1 Maximum Tensile Stress

Figure 5 shows stress distribution σ_θ at the shrink fitting ratio $\delta/d = 3.0\times10^{-4}$. Figure 5(a) shows the stress $\sigma_{\theta s}$ due to shrink fitting and Fig.5 (b) shows maximum stress distribution $\sigma_{\theta\max}\left(=\sigma_{\theta s}+\sigma_{\theta b}\right)$ due to load distribution $w = 100N/mm$ after shrink fitting. As shown in Fig.5, the maximum tensile stress at point A is $75.2MPa$ while shrink fitting. It becomes $85.6MPa$ by applying the distribution load after shrink fitting. In other words, $\sigma_{\theta b}$ increases by $10.4MPa$.

Figure 6 shows stress distribution σ_z at the shrink fitting ratio $\delta/d = 3.0\times10^{-4}$. Figure 6 (a) shows the stress σ_{zs} due to shrink fitting and Fig.6 (b) shows maximum stress distribution $\sigma_{z\max}\left(=\sigma_{zs}+\sigma_{zb}\right)$ due to load distribution $w = 100N/mm$ after shrink fitting. As shown in Fig.6, the maximum tensile stress at point B is $34.5MPa$ while shrink fitting. It becomes $54.5MPa$ by applying the distribution load after shrink fitting. In other words, σ_{zb} increases by $20.0MPa$.

It is found that the maximum tensile stress appears at point A as σ_θ. In this study we will focus on reducing the maximum tensile stress σ_θ at A with varying geometrical conditions.

Table1 Material Properties

	Young's modulus [GPa]	Poisson's ratio	Tensile strength [MPa]	Fracture toughness [MPa$\sqrt{}$m]
Ceramics	300	0.28	500	7.7
Cemented Carbide	500	0.24	1000	20
Steel	210	0.3	600	100

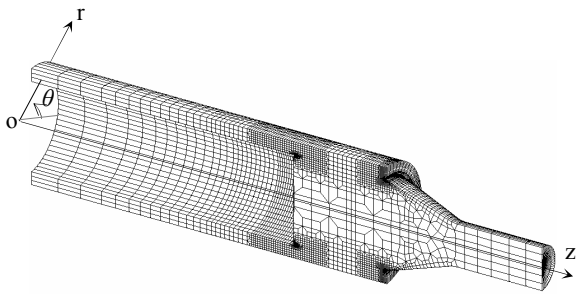

Fig.4 FEM mesh

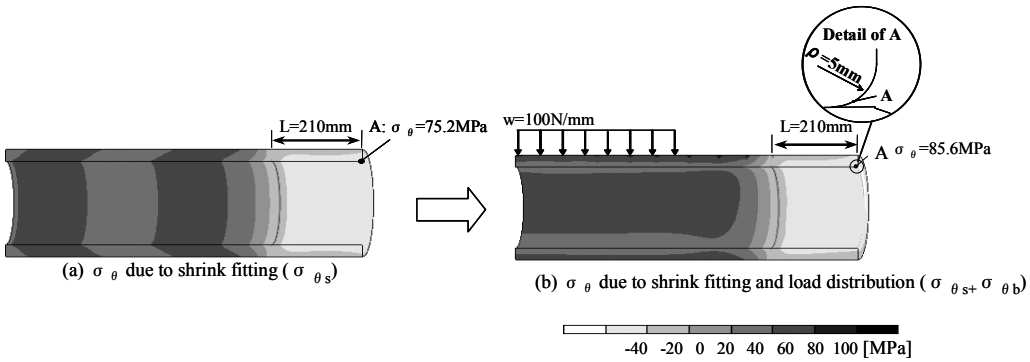

Fig.5 Stress distribution σ_θ when $\delta/d=3.0\times10^{-4}$

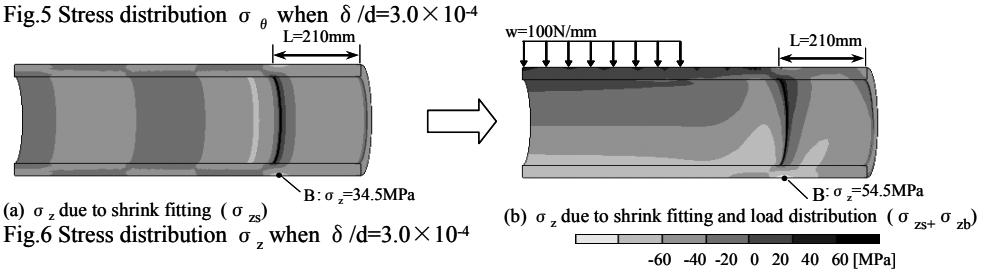

Fig.6 Stress distribution σ_z when $\delta/d=3.0\times10^{-4}$

3.2 Effect of Shrink Fitting Ratio and Bending Moment upon the Maximum Tensile Stress $\sigma_{\theta\max}$

Figure 7 illustrates effects of shrink fitting ratio δ/d upon the stresses $\sigma_{\theta s}$, $\sigma_{\theta\max}$, $\sigma_{\theta b}$. Figure 7 (a) shows the $\sigma_{\theta s}$, $\sigma_{\theta\max}\left(=\sigma_{\theta s}+\sigma_{\theta b}\right)$ vs. δ/d relationship when the load distribution $w=100N/mm$ is applied after shrink fitting. To clarify the effect of load distribution, Fig.7 (b) shows the $\sigma_{\theta b}=\sigma_{\theta\max}-\sigma_{\theta s}$ vs. δ/d relationship when the load distribution $w=100N/mm$ is applied. From Fig.7 (b) it is found that $\sigma_{\theta\max}$ has a minimum value at $\delta/d=0.50\times10^{-4}$. When $\delta/d\geq1.5\times10^{-4}$, $\sigma_{\theta s}$ increases linearly with increasing δ/d. On the other hands, $\sigma_{\theta b}$ decreases with increasing δ/d, and becomes constant when $\delta/d\geq1.5\times10^{-4}$. Detail investigations reveal that the constant value $\sigma_{\theta b}=10.5MPa$ coincides with the value when the shaft and sleeve are perfectly bonded as a unit body. From Fig.7 (b), it is found that the large δ/d reduces the contact stress $\sigma_{\theta b}$ by gripping the shaft tightly. It may be concluded that $\sigma_{\theta\max}=\sigma_{\theta s}+\sigma_{\theta b}$ has a minimum value at a certain value of δ/d. This is because with increasing δ/d the stress $\sigma_{\theta s}$ increases monotonously but $\sigma_{\theta b}$ decreases and becomes constant.

3.3 The Effect of Fitted Length L on $\sigma_{\theta s}$, $\sigma_{\theta\max}$, $\sigma_{\theta b}$

Figure 8 (a) shows $\sigma_{\theta s}$, $\sigma_{\theta\max}\left(=\sigma_{\theta s}+\sigma_{\theta b}\right)$ vs. δ/d relation when the load distribution $w=100N/mm$ is applied after shrink fitting for different fitted length L. Here, we assume the fitted length $L=100mm$, $150mm$, $210mm$. Small values of L are desirable for the maintenance because exchanging the sleeve is easier for smaller L. Figure 8 (b) shows $\sigma_{\theta b}$ vs. δ/d relation when the load distribution $w=100N/mm$ is applied. When shrink fitting ratio $\delta/d\geq2.0\times10^{-4}$, $\sigma_{\theta b}$ becomes constant and independent of δ/d. When $\delta/d\geq2.0\times10^{-4}$, the shafts and sleeve can be treated as a unit body bonded perfectly.

From Fig.8 (a), it is found that $\sigma_{\theta\max}$ has a minimum value $60.5MPa$ at $\delta/d=1.8\times10^{-4}$ when L=100mm. Similarly, it is found that the optimum shrink fitting

ratio is $\delta/d = 1.2\times10^{-4}$ when $L = 150mm$, and also $\delta/d = 5.0\times10^{-5}$ when $L = 210mm$. When shrink fitting ratio $\delta/d \geq 2.0\times10^{-4}$, $\sigma_{\theta b}$ becomes constant $10.5MPa$ independent of δ/d.

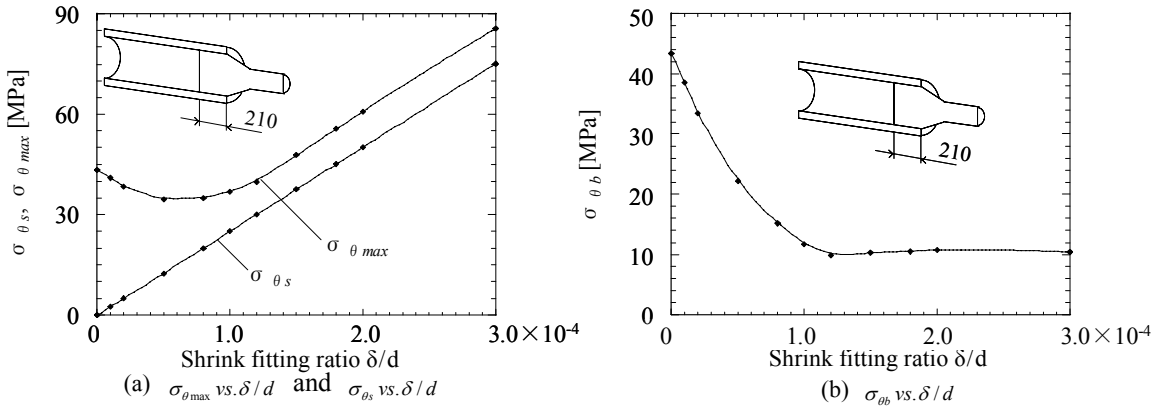

(a) $\sigma_{\theta\max}$ $vs.\delta/d$ and $\sigma_{\theta s}$ $vs.\delta/d$ (b) $\sigma_{\theta b}$ $vs.\delta/d$

Fig.7 σ_θ $vs.\delta/d$ when L= 210mm

($\sigma_{\theta\max} = \sigma_{\theta s} + \sigma_{\theta b}$, $\sigma_{\theta s}$: Stress due to shrink fitting, $\sigma_{\theta b}$: Stress due to load distribution)

3.4 The Effect of Materials Difference on $\sigma_{\theta s}$, $\sigma_{\theta\max}$, $\sigma_{\theta b}$

Figure 9 shows $\sigma_{\theta s}$, $\sigma_{\theta\max}$, $\sigma_{\theta b}$ vs. δ/d relation for different materials of sleeve. As shown in Fig.9 (b), the maximum tensile stress of cemented carbide is larger than those of ceramics and steel at the same value of δ/d. This is because the Young's modulus of cemented carbide $E = 500MPa$ is larger than the ones of ceramics $E = 300MPa$, and steel $E = 210MPa$ (see Table 1).

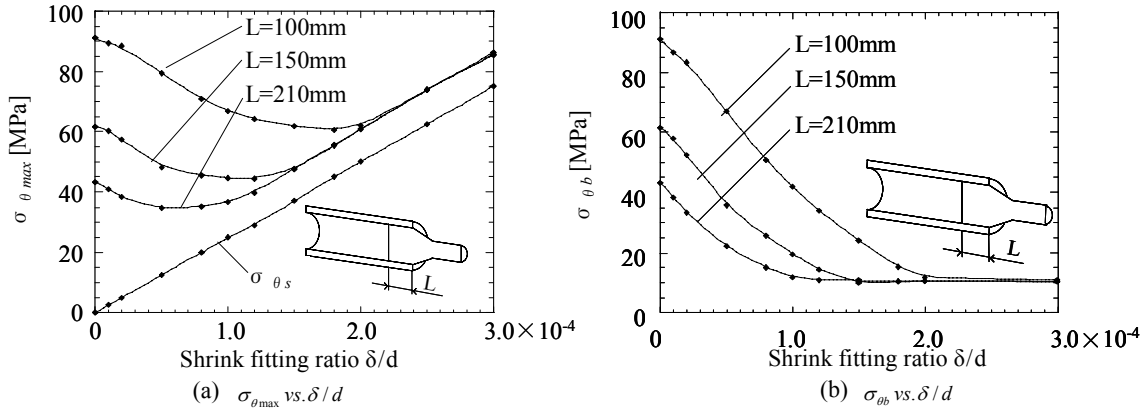

(a) $\sigma_{\theta\max}$ $vs.\delta/d$ (b) $\sigma_{\theta b}$ $vs.\delta/d$

Fig.8 σ_θ $vs.\delta/d$ when L=100mm, 150mm, 210mm

($\sigma_{\theta\max} = \sigma_{\theta s} + \sigma_{\theta b}$, $\sigma_{\theta s}$: Stress due to shrink fitting, $\sigma_{\theta b}$: Stress due to load distribution)

From Fig. 9(c), $\sigma_{\theta b}$ becomes constant when δ/d is large. The constant values are $\sigma_{\theta b}$=9.2MPa for steel, $\sigma_{\theta b}$=10.5MPa for ceramics and $\sigma_{\theta b}$=11.4MPa for cemented carbide. These results coincide with the case when the shafts and sleeve are perfectly bonded. It is seen that $\sigma_{\theta b}$ becomes constant at a smaller value of δ/d if the Young's modulus becomes larger. This is because larger Young's modulus reduces the maximum contact stress by tightening the shafts stronger even under the same value of δ/d.

3.5 The Effect Radius Curvature ρ on $\sigma_{\theta s}, \sigma_{\theta \max}, \sigma_{\theta b}$

In the previous discussion, the radius curvature ρ at the edge of sleeve is always assumed as $\rho = 5mm$. However, the values of $\sigma_{\theta s}$, $\sigma_{\theta \max}$, $\sigma_{\theta b}$ may be changed depending on the radius curvature ρ because $\sigma_{\theta \max}$ appears at point A in the circular arc part at the edge of sleeve. As shown in Fig. 10, therefore, the effect of radius curvature is analyzed with varying $\rho = 5mm$, $10mm$, $20mm$, and $30mm$. The relationships between the shrink fitting ratio δ/d and $\sigma_{\theta s}$, $\sigma_{\theta \max}$, $\sigma_{\theta b}$ are shown in Fig.11. From Fig.11 (a) and Fig.11 (b) it is found that the maximum stresses $\sigma_{\theta s}$, $\sigma_{\theta \max}$ increase with decreasing the radius ρ. For the large values of δ/d, the stress $\sigma_{\theta b}$ becomes constant at the same value of δ/d independently of ρ. At the fixed value of $\delta/d = 3.0\times10^{-4}$, for example $\sigma_{\theta \max} = 85.6MPa$ when $\rho = 5mm$ but $\sigma_{\theta \max} = 69.1MPa$ when $\rho = 30mm$.

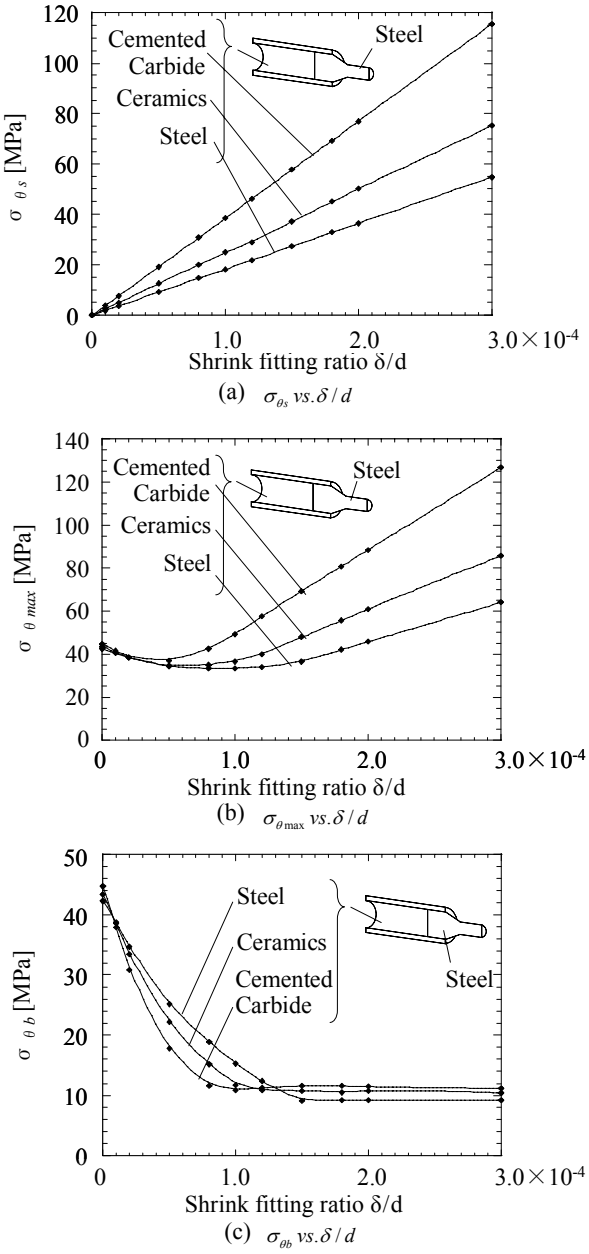

Fig.9 σ_θ $vs.\delta/d$ when Steel, Ceramics, Cemented Carbide are used as the sleeve
($\sigma_{\theta \max} = \sigma_{\theta s} + \sigma_{\theta b}$, $\sigma_{\theta s}$: Stress due to shrink fitting, $\sigma_{\theta b}$: Stress due to load distribution)

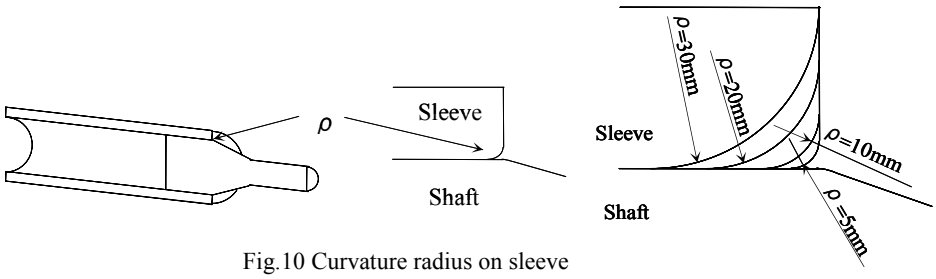

Fig.10 Curvature radius on sleeve

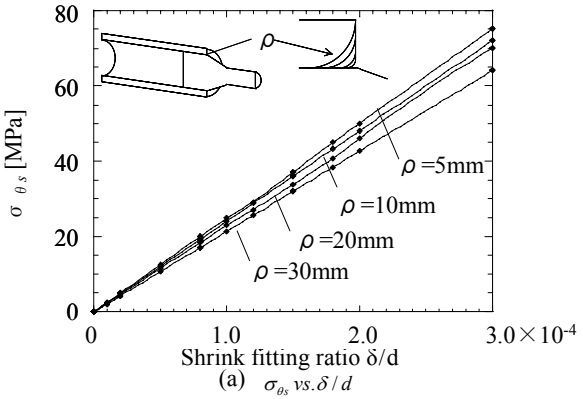

(a) $\sigma_{\theta s}$ *vs.* δ / d

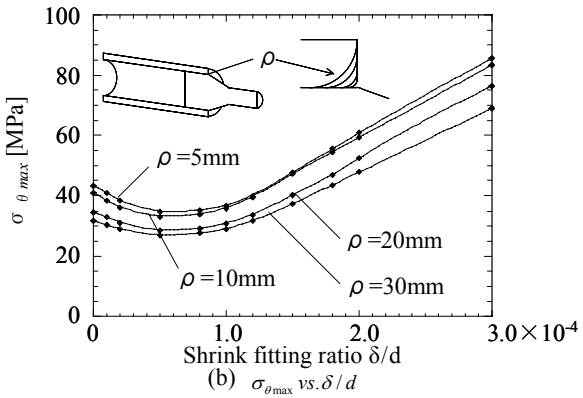

(b) $\sigma_{\theta \max}$ *vs.* δ / d

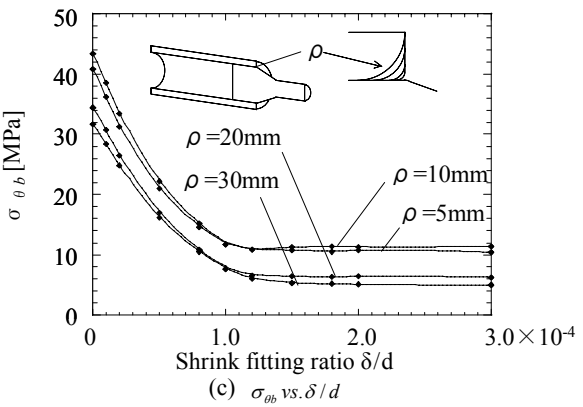

(c) $\sigma_{\theta b}$ *vs.* δ / d

Fig.11 σ_θ *vs.* δ / d when $\rho = 5,10,20,30mm$
($\sigma_{\theta \max} = \sigma_{\theta s} + \sigma_{\theta b}$, $\sigma_{\theta s}$: Stress due to shrink fitting, $\sigma_{\theta b}$: Stress due to load distribution)

From Fig. 11(c), it is seen that $\sigma_{\theta b}$ becomes larger when δ / d is smaller. However, when

$\delta/d \geqq 1.5\times10^{-4}\,\sigma_{\theta b}$ for ρ=10mm is larger than $\sigma_{\theta b}$ for ρ=5mm.

3.6 The Effect of Diameter D on $\sigma_{\theta s}$, $\sigma_{\theta\max}$, $\sigma_{\theta b}$

Figure 12 shows the relationships between shrink fitting ratio δ/d and $\sigma_{\theta s}$, $\sigma_{\theta\max}$, $\sigma_{\theta b}$ with varying the outside diameter of sleeve as $D=270mm$, $405mm$ and $540mm$. Here, we assume a ceramics sleeve has a fitted length $L=210mm$, radius of curvature $\rho=5mm$, and thickness of the sleeve $(D-d)/2=30mm$. Also, we calculate magnitudes of load distribution w so as to produce the same value of nominal bending stress σ_{zn} from

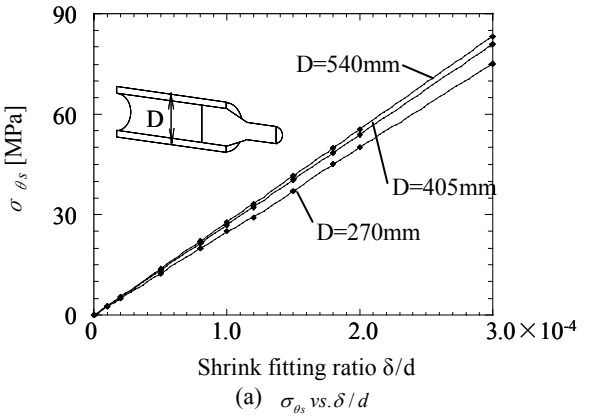

(a) $\sigma_{\theta s}$ $vs.\delta/d$

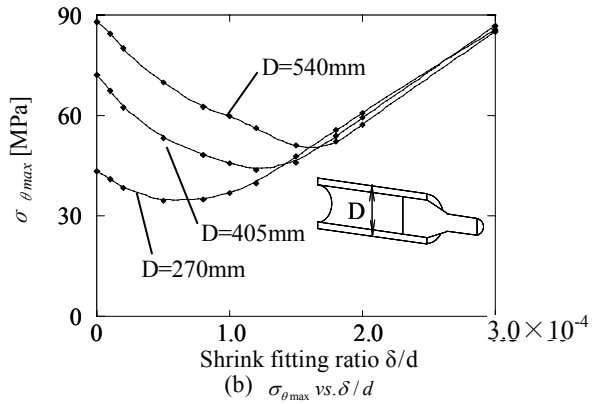

(b) $\sigma_{\theta\max}$ $vs.\delta/d$

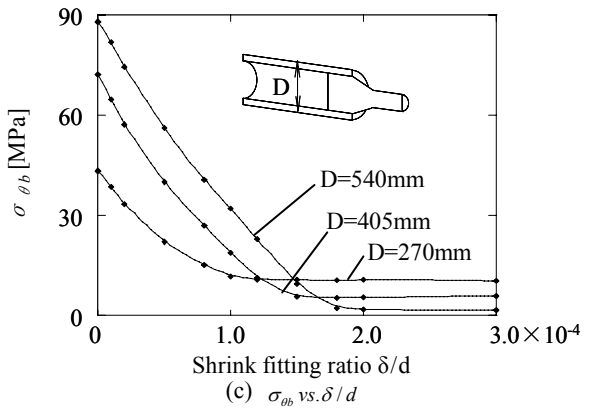

(c) $\sigma_{\theta b}$ $vs.\delta/d$

Fig.12 σ_θ $vs.\delta/d$ when D=270, 405, 540mm
($\sigma_{\theta\max}=\sigma_{\theta s}+\sigma_{\theta b}$, $\sigma_{\theta s}$: Stress due to shrink fitting, $\sigma_{\theta b}$: Stress due to load distribution)

Eq. (1). Then, we have $w = 100N/mm$ for $D = 270mm$, $w = 243N/mm$ for $D = 405mm$, $w = 450N/mm$ for $D = 540mm$. The nominal bending stress is expressed by

$$\sigma_{zn} = \frac{32M}{\pi\left(D^3 - d^3\right)} \tag{1}$$

where

D : outside diameter of sleeve (mm)

d : inner diameter of sleeve (mm)

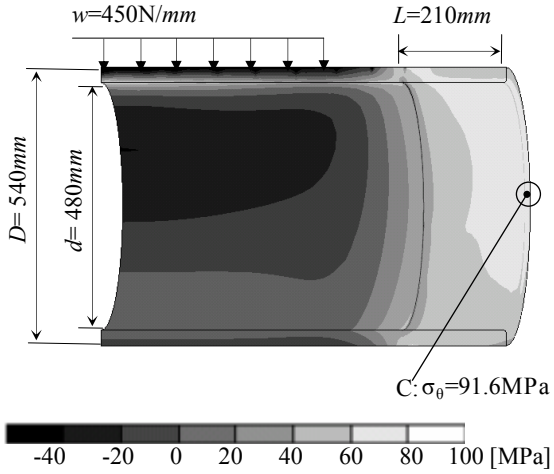

Fig.13 σ_θ due to shrink fitting and load distribution when $\delta/d = 3.0\times10^{-4}$

M : bending moment (Nmm)

Figure 12(b) shows that $\sigma_{\theta\max}$ increases with increasing the outer diameter of the sleeve when δ/d is small. With increasing the diameter D, a minimum value of $\sigma_{\theta\max}$ is appearing at a larger value of δ/d. Figure 12(b) is closely related to Fig.8 (a), where the fitted length L is changed under a constant D. In other words, increasing D under a fixed L in Fig.12 (b) is found to be almost equivalent to decreasing L under a fixed D in Fig.8 (a).

From Fig.12(c), it is seen that for large values of δ/d, $\sigma_{\theta b}$ becomes constant independently of δ/d. The constant values are $\sigma_{\theta b} = 10.4MPa$ for D=270mm, $\sigma_{\theta b} = 5.5MPa$ for $D = 405mm$, and $\sigma_{\theta b} = 1.9MPa$ for $D = 540mm$. Further investigations reveal that those constant values coincide with the values when the shaft and sleeve are perfectly bonded as a unit body. With increasing the outer diameter D, $\sigma_{\theta b}$ becomes constant under larger values of δ/d.

Figure 13 shows a stress distribution σ_θ due to the load distribution $w = 450N/mm$ after shrink fitting when $D = 540mm$ with $\delta/d = 3.0\times10^{-4}$. Care should be taken for the large diameter D because the maximum stress $91.6MPa$ appears at point C instead of A in Fig.5 differently from other cases when $\delta/d \geqq 1.0\times10^{-4}$.

4. Conclusions

Hot conveyed strips induce wear on the steel roller surface in short periods. To reduce maintenance cost for exchanging the rollers, in this study, a new structure is considered where a ceramics sleeve connected with short steel shafts at both ends. Stress analysis was performed with the application of the finite element method; then several geometrical conditions were investigated, such as fitted length L, radius curvature ρ at end of the sleeve, outer diameter D of the sleeve. The conclusions can be made in the following way.

1. The maximum tensile is appearing at the end of the sleeve as $\sigma_{\theta\max}$. The stress $\sigma_{\theta\max}$ may be expressed by $\sigma_{\theta\max} = \sigma_{\theta s} + \sigma_{\theta b}$ where $\sigma_{\theta s}$ is a shrink fitting stress and $\sigma_{\theta b}$ is a stress due to load distribution. For example, the maximum value $\sigma_{\theta\max} = 85.6MPa$ appears under the load w=100N/mm after shrink fitting. Here, $\sigma_{\theta s} = 75.2MPa$, $\sigma_{\theta b} = \sigma_{\theta\max} - \sigma_{\theta s} = 10.4MPa$ when the fitted length $L = 210mm$, shrink fitting ratio $\delta/d = 3.0\times10^{-4}$, radius curvature $\rho = 5mm$, and outer diameter $D = 270mm$ (see Fig.5).
2. For large values of δ/d, $\sigma_{\theta b}$ becomes constant independently from δ/d. The constant value coincides with the results when the shafts and sleeve are perfectly bonded. In other words, if δ/d is large enough, the shafts and sleeve can be treated as a unit body.
3. For small values of δ/d, the maximum stress $\sigma_{\theta\max}$ becomes larger because large contact forces may appear between the sleeve and shafts, especially for small L. Suitably larger values of δ/d may reduce $\sigma_{\theta\max}$ effectively. In other words, $\sigma_{\theta\max}$ takes a minimum value at a certain value of δ/d.
4. The effect of material difference of the sleeve was considered. Under small values of δ/d, a larger Young's modulus of the sleeve may reduce $\sigma_{\theta b}$ because the sleeve clamps the shafts more tightly and reduces the magnitude of contact forces. On the other hand, large values of δ/d with larger Young's modulus of sleeve may increase the value of $\sigma_{\theta s}$.
5. With increasing the radius ρ at the end of sleeve, the maximum stress $\sigma_{\theta\max}$ decreases. The stress $\sigma_{\theta b}$ becomes constant at almost the same value of δ/d independent of ρ.
6. Care should be taken for large diameters D because the maximum stress σ_{θ} may appear at a different position. Increasing diameter D under a fixed fitted length L is almost equivalent to decreasing L under a fixed D.

References

(1) Miki, E., High Corrosion Resistance and Cost Reduction by Spraying Methods, *Plant Engineer*, Vol.21, No.1 1989 (in Japanese).
(2) Iwata, T. and Mori, H.,Material Choice for Hot Run Table Roller, *Plant Engineer*, Vol.15, No.6 1983 (in Japanese).
(3) Harada, S., Noda, N., Uehara, O. and Nagano, M., Tensile Strength of Hot Isostatic Pressed Silicon Nitride and Effect of Specimen Dimension, *Transactions of the Japan Society of Mechanical Engineering*, Vol.57, No.539 1991.
(4) Kobayashi, H., and Kawakubo, T., Fatigue –Difference between ceramics and metal–, *Journal of the Japan Institute of Metals*, Vol.27, No.10 1988.